IIOAB JOURNAL
ISSN: 0976-3104

CHARACTERIZATION OF COPPER(II)-ZIRCONIUM(IV)-IMIDAZOLATE FRAMEWORK SYNTHESIZED BY HYDROTHERMAL METHOD

Sonam Goyal*, Maizatul Shima Shaharun, Chong Fai Kait

Dept. of Fundamental and Applied Sciences, Universiti Teknologi PETRONAS, 32610 Seri Iskandar, Perak, MALAYSIA

ABSTRACT

Copper(II) imidazolate and two different mass ratio of copper(II) - zirconium(IV) bimetallic imidazolate (2Cu:1Zr and 1Cu:2Zr) were synthesized by hydrothermal method using metal sulphates in aqueous solution. The metal imidazolate frameworks were characterized by field emission scanning electron microscope (FESEM), thermogravimetry (TG), ultraviolet-visible spectroscopy (UV-Vis) and N_2 adsorption–desorption. The addition of zirconia increased the surface area of the metal organic frameworks and also makes it thermally stable up to 250˚C. The incorporation of zirconia into the copper(II) imidazolate improves the visible light absorbance. The band gap of 2:1 and 1:2 mass ratio of copper(II) - zirconium(IV) imidazolate increased to 2.70 eV and 3.28 eV, respectively, with more absorbance in the visible region compared to copper(II) imidazolate with 1.65 eV.

KEY WORDS

Photocatalyst, Copper, Zirconia, Hydrothermal, Imidazolate Framework

Received: 13 Oct 2016
Accepted: 16 Nov 2016
Published: 1 Dec 2016

***Corresponding Author**
Email: sonamgoyal2014@gmail.com

INTRODUCTION

The metal–organic frameworks (MOFs), which are self-assembled by the coordination of metal cations/groups with organic linkers, have potential applications in catalysis, gas storage, sensors, nonlinear optics, and separation. Due to the high surface area of MOFs, high metallic deposits are observed, and the limited micropore circulation leads to monodisperse nanometric metallic groups [1][16]. Contrasted with different sorts of metal–organic structure materials, ZIFs frequently exhibited better thermal and chemical stabilities [2-4]. Today's main issue is worldwide ecological increasing temperature, which is due to burning of fossil fuels causes rising CO_2 level in the atmosphere. Photocatalytic transformation of CO_2 under ambient conditions offers an attractive solution to reduce greenhouse gasses. Numerous metal oxide semiconductors, for example, ZnO, CdS [5], TiO_2 [6] and Zn_2GeO_4 [7] etc. have been explored for photoreduction of CO_2 into fuels. However, the economics of the CO_2 conversion process is low. This is mainly due to the recombination of photogenerated electron–hole, low usage proficiency of sun-powered vitality and low adsorption of CO_2 [8, 9]. Specifically, expanding the surface area of photocatalysts is a powerful approach to provide more receptive sites and superior adsorption properties and therefore enhance the photocatalytic reaction. Metal–organic frameworks(MOFs) have drawn great attention for their potential use as adsorbents and catalysts because of the high surface area, huge pore size, tunable nanometer-scale holes, and chemically modify ability [10][15].

Copper(II) imidazolate has been developed by hydrothermal method [11]. In this study, the same method was used to synthesize copper(II) imidazolate and copper(II) – zirconium(IV) imidazolate (CuZrIm 2:1 and CuZrIm 1:2) to study the influence of zirconia on the physiochemical properties of copper(II) imidazolate (CuIm). The physiochemical properties were studied by using a field emission scanning electron microscope (FESEM), thermogravimetry (TG), ultraviolet-visible spectroscopy (UV-Vis) and N_2 adsorption–desorption.

EXPERIMENTAL

Synthesis of copper(II) imidazolate (CuIm)

0.25 g imidazole (3.67 mmol) in 15 mL H_2O was added to 0.5 g $CuSO_4.5H_2O$ (2 mmol) in 3 mL of H_2O, and then 4M NH_3 (aq) was added to produce a 25 mL of solution. The mixture was poured into Teflon-lined stainless steel autoclave and hydrothermally treated at 110˚C for 48 h. The solid product collected by filtration and washed with deionized water for 3–4 times. The sample was finally dried at 80˚C overnight in an oven.

Synthesis of copper(II)-zirconium(IV) imidazolate (CuZrIm 2:1 and 1:2)

In synthesizing, CuZrIm 2:1, imidazole (0.25 g, 3.67 mmol) in 15 mL water was added to stirred suspension of $CuSO_4.5H_2O$ (0.5 g, 2 mmol) and $Zr(SO_4)_2.H_2O$ (0.25 g, 0.83 mmol) in 3 mL of H_2O. As for CuZrIm 1:2, 15 ml of imidazole solution (0.25 g, 3.67 mmol) was mixed to mixture of $CuSO_4.5H_2O$ (0.25 g, 1 mmol) and $Zr(SO_4)_2.H_2O$ (0.50 g, 1.65 mmol) and bringing the volume up to 25 mL with 4 M NH_3 of both solutions. The mixture was hydrothermally treated into the Teflon autoclave, which keeps it in an oven at 110˚C for 48 h. The product filtered, washed with deionized water for 3-4 times, and then dried overnight in an oven at 80˚C.

IIOAB JOURNAL
ISSN: 0976-3104

CHARACTERIZATION

The morphology, and elemental compositions of the catalyst were studied using field emission scanning electron microscope-energy dispersive X-ray (JEOL6340). The surface area, and pore volume were analyzed using gas adsorption device ASAP 2020 (Micrometrics Instrument). The materials were degassed at 200˚C for 2h under 50mTorr vacuum. The surface area calculation was explained by Brunauer-Emmett-Teller (BET) isotherm method, while for micro and mesopores evaluation utilized Horwarth-Kavazoe, and BJH methods, respectively [12]. The UV-Vis spectroscopy in the 200-800 nm was measured with an Agilent Cary 100 UV-Vis Spectrophotometer and diffuse reflectance spectroscopy is used to determine the optical absorption in the visible light region. A thermogravimetric analyzer (TGA) was used to measure weight changes of the sample, when heated under nitrogen flow with a heating rate of 20˚C/min from room temperature to 500˚C. The examining TGA was done on a Perkin Elmer Pyris 1, which exhibits the thermal stability of the materials.

RESULTS AND DISCUSSION

The thermal stability of the synthesized materials are shown in [Fig. 1]. The comparing results appeared in [Fig. 1]. The weight loss started at 280˚C and continued up to 600˚C in CuIm.

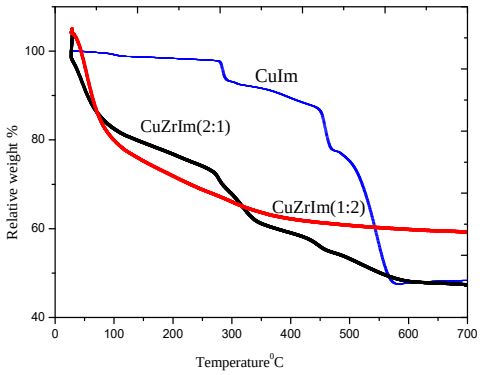

Fig. 1: Thermo gravimetric analysis of metal imidazolate frameworks.

Addition of zirconia into CuIm, shows higher thermal stability. CuZrIm 2:1 shows weight loss at 80˚C, which means sample contains water molecule, continued to 600˚C, and then 49% remain same as CuIm. Beside this, an increment of zirconia (CuZrIm 1:2) exhibits weight loss from 80˚C to 100˚C water loss from sample and then weight loss up to 300˚C and then 65% remains. All the above results show that CuZrIm 1:2 indicates higher thermal stability.

The diffuse reflectance UV−vis spectra were used to determine optical properties of the three metal imidazolate frameworks. [Fig. 2] illustrates the optical absorbance of the three metal imidazolate. Band gap energies were determined by the DR-UV-vis. For materials, the band gap energy in this investigation could be assessed from a plot of $(\alpha hv)^2$ versus photon energy hv/eV. As presented in [Fig. 3], the immediate band gap for CuIm, CuZrIm 2:1 and CuZrIm 1:2 are found to be 1.65, 2.70, and 3.28 eV, respectively.

IIOAB JOURNAL
ISSN: 0976-3104

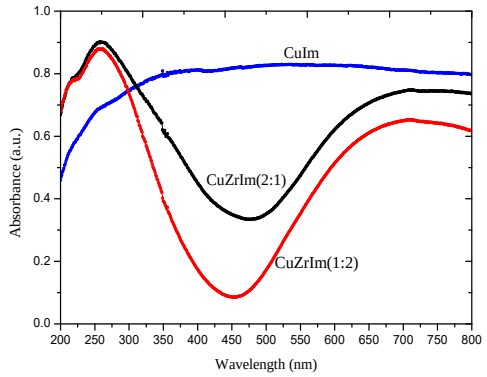

Fig. 2: Diffuse reflectance UV-vis spectra of CuIm, CuZrIm 2:1 and CuZrIm 1:2.

The band gap of zirconia is larger (5-7 eV). Therefore, an incorporation of a larger band gap of zirconia into CuIm results in shifting of the band gap to lower energies. As can be seen, both CuZrIm show their optical absorbance edges between 400 and 550 nm, which indicates absorbance in the visible light region. The results suggest that CuZrIm 2:1 and CuZrIm 1:2 can be photoexcited to create more electron−hole pairs than CuIm under visible light absorbance which could leads to higher photocatalytic efficiency.

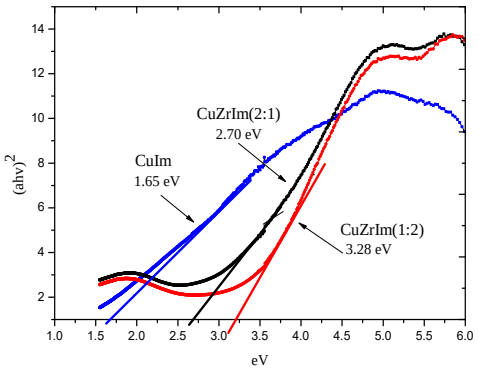

Fig. 3: Diffuse reflectance spectra for band gap measurement of CuIm, CuZrIm 2:1 and CuZrIm 1:2.

The impact of zirconia on the morphology of the CuIm was studied using FESEM. The FESEM micrograph of the samples are shown in [Fig. 4]. It can be seen from [Fig. 4], that the surface characteristics of CuIm were significantly changed with the addition of Zr. The surface morphological exhibits different particle shapes was as illustrated in [Fig. 4]. CuZrIm 2:1 and 1:2 exhibit smaller and uniform particle size. However, more particles agglomerated to form crystal-like structure with the addition of more Zr.

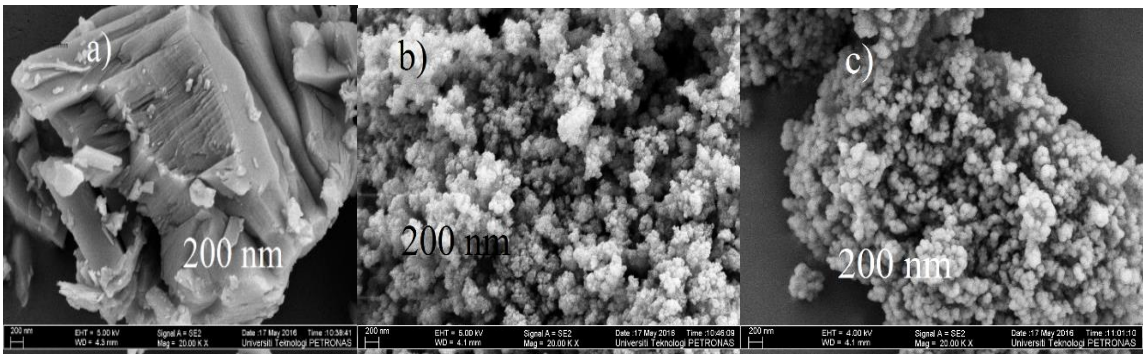

ISSN: 0976-3104

Fig. 4: FESEM images of (a) CuIm (b) CuZrIm 2:1 and (c) CuZrIm 1:2.

The average diameters increased from ca. 120 to 170 nm by increasing the Zr^{4+} doping percentage in the nanocrystals. This confirms that fewer nuclei were formed upon addition of imidazole. Cu and Zr-doped imidazolate crystals initially formed grew further with increase addition of single monomeric imidazole, solvanating Zr^{4+}, and Cu^{2+} species until the framework is formed. Regardless of the doping percentage, FESEM images showed rather small and monodispersed nanoparticles with a well-defined truncated rhombic dodecahedron structure, which is the typical imidazolate framework morphology.

[Fig. 5] outlines the FESEM mapping, and EDX of the CuIm and CuZrIm 1:2 sample demonstrating the metal distribution on the surface of support. Every component present in the sample structure is finely distributed by dots with a specific color. It can be seen from the [Fig. 5], that Cu species are homogeneously distributed. The EDX examination of CuZrIm 1:2 showed that Cu, Zr, C, and O were the main 4 components observed on the surface of sample.

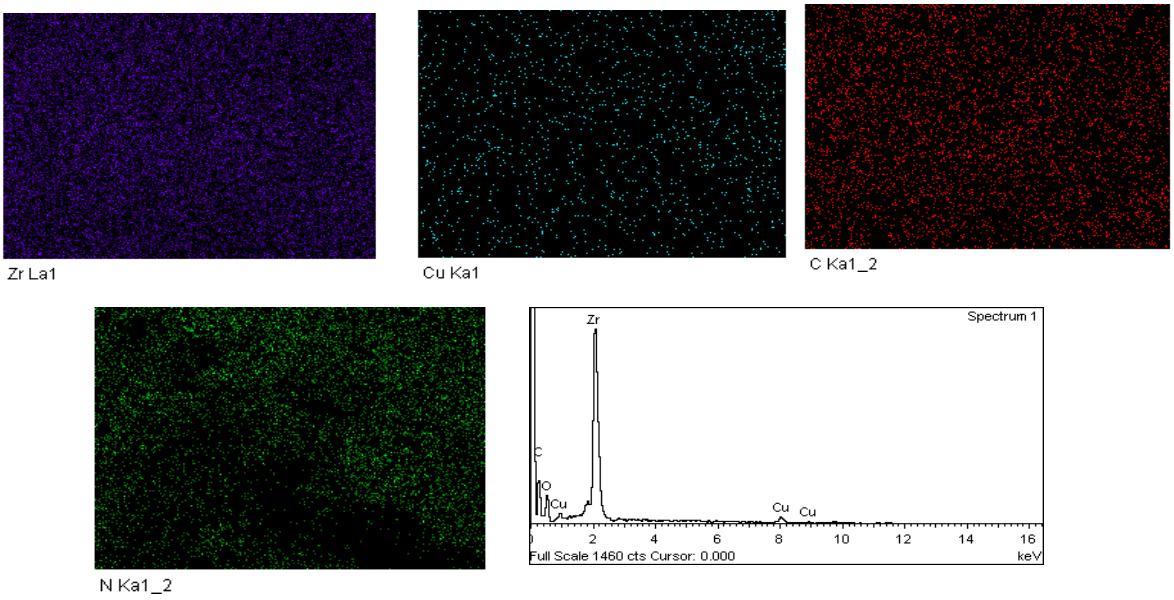

Fig. 5: Representative elemental apping of CuIm and CuZrIm 1:2.

As shown in [Fig. 6], CuIm presents a combination of type III and IV isotherm [13] at relative pressures below 0.9. This is due to the low surface area, where isotherm relates to samples with a low affinity for the adsorbate (N_2) which exhibits a mixture of macroporous and mesoporous characteristics. This exhibit type IV at high relative pressure.

Both CuZrIm 2:1 and CuZrIm 1:2 give the characteristic of mesoporous solids because it shows hysteresis loop type H-1 adsorption isotherms with type IV [Fig. 6]. Each isotherm shows a distinct hysteresis loop, which is associated with capillary condensation taking place in the mesoporous. It shows that the photocatalyst is mainly mesopores. Sharp inflections in-between P/P^o of 0.9–1.0 and typical H-1 type hysteresis loop are observed for both CuZrIm [12].

IIOAB JOURNAL
ISSN: 0976-3104

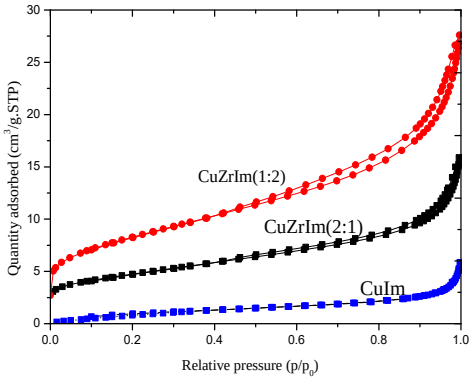

Fig. 6: Hysteresis loops of different catalyst.

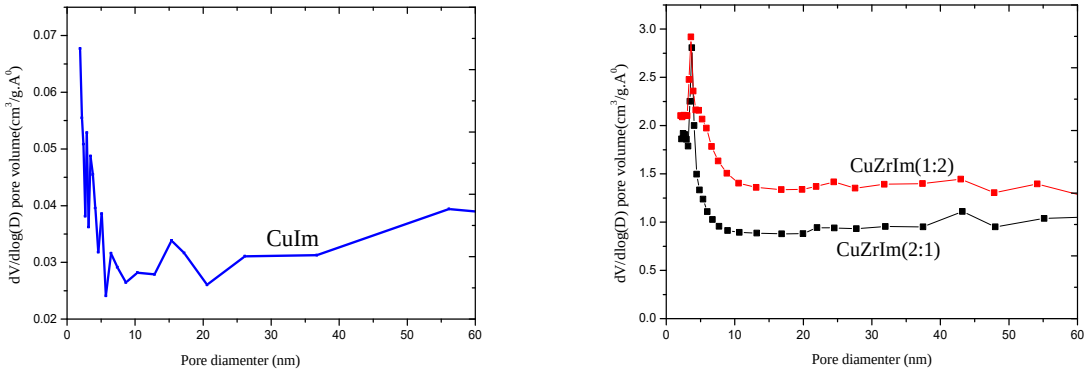

Fig. 7: Pore-size distributions with average pore sizes.

The surface area of the materials was executed by nitrogen adsorption. [Table 1] shows nitrogen adsorption properties of the three metal organic frameworks. As indicated by the Brunauer–Emmett–Teller (BET), the BET surface ranges of CuIm, CuZrIm 2:1 and CuZrIm 1:2 were computed to be 4.11, 120.33 and 234.15 m^2/g, respectively. It gives proof that increment of zirconia loading shows the highest surface area and pore volume of the sample but the average diameter of pores is smaller. It is evident from [Fig. 7] that CuIm and both CuZrIm (2:1 and 1:2) has a narrow pore size distribution. CuIm has average pore size distribution at 2.0 nm and both CuZrIm has average pore-size distribution at 5.0 nm. Most of the pores are in mesoporous region (2 nm - 10 nm). It is suggested that the high surface:volume ratio of the CuZrIm results in higher surface-energy stabilisation as opposed to the CuIm phase [14].

Table 1: Specific area and pore volume

Catalyst	Surface Area (m^2/g)	Pore Volume (cm^3/g)	Average Diameter of Pore (nm)
CuIm	4.1197	0.007848	7.61987
2:1CuZrIm	120.3357	0.201338	6.50423
1:2CuZrIm	234.1586	0.365294	6.06503

CONCLUSION

Copper(II) imidazolate and copper(II)-zirconia(IV) bimetallic imidazolate (2:1 and 1:2 mass ratios) were synthesized by hydrothermal method using metal sulphates in mild aqueous conditions with high yields. The physicochemical properties of the photocatalysts were examined by different characterization techniques. The thermal stability, surface area and pore volume of both CuZrIm is higher than CuIm. It is found that the band gap of CuZrIm 2:1 and CuZrIm 1:2 increased to 2.70 eV and 3.28 eV, respectively with more absorbance in the visible region compared to copper(II) imidazolate framework.

IIOAB JOURNAL
ISSN: 0976-3104

CONFLICT OF INTEREST

There is no conflict of interest.

ACKNOWLEDGEMENTS

Financial assistant from Universiti Teknologi PETRONAS (UTP) and Ministry of Higher Education Malaysia, FRGS No: FRGS/2/2013/SG01/UTP/02/2 is gratefully acknowledged. The authors acknowledge use of facilities within the UTP Centralized Analytical Laboratory (CAL).

FINANCIAL DISCLOSURE

None

REFERENCES

[1] Zhao Y, Zhang J, Song J, , et al.[2011] Ru nanoparticles immobilized on metal–organic framework nanorods by supercritical CO 2-methanol solution: highly efficient catalyst, Green Chemistry, 13:2078-2082.
[2] Banerjee R, Phan A, Wang B, et al.[2008] High-throughput synthesis of zeolitic imidazolate frameworks and application to CO2 capture, Science, 319:939-943,
[3] Phan A, Doonan CJ, Uribe-Romo FJ, Knobler CB, O'keeffe M, Yaghi OM. [2010] Synthesis, structure, and carbon dioxide capture properties of zeolitic imidazolate frameworks, cc. Chem. Res, 43:58-67.
[4] Pan Y, Liu Y, Zeng G, Zhao L, Lai Z. [2011] Rapid synthesis of zeolitic imidazolate framework-8 (ZIF-8) nanocrystals in an aqueous system, Chemical Communications, 47: 2071-2073,
[5] Inoue T, Fujishima A, Konishi S, Honda K.[1979] Photoelectrocatalytic reduction of carbon dioxide in aqueous suspensions of semiconductor powders, Nature, 277:637-638.
[6] Wang WN, An WJ, Ramalingam B, Mukherjee S, , et al.[2012] Size and structure matter: enhanced CO_2 photoreduction efficiency by size-resolved ultrafine Pt nanoparticles on TiO_2 single crystals, Journal of the American Chemical Society, 134: 11276-11281.
[7] Liu Q, YZhou , Kou J, Chen X, Tian Z, Gao J, et al.[2010] High-yield synthesis of ultralong and ultrathin Zn2Ge04 nanoribbons toward improved photocatalytic reduction of CO2 into renewable hydrocarbon fuel, Journal of the American Chemical Society, 132:14385-14387.
[8] Hoffmann MR, Moss JA, Baum MM.[2011] Artificial photosynthesis: semiconductor photocatalytic fixation of CO2 to afford higher organic compounds," Dalton Transactions, 40:5151-5158.
[9] Q Liu, Z.-X. Low, L Li, A. Razmjou, K Wang, J Yao, et al.[2013] ZIF-8/Zn 2 GeO 4 nanorods with an enhanced CO2 adsorption property in an aqueous medium for photocatalytic synthesis of liquid fuel, Journal of Materials Chemistry A, 1:11563-11569.
[10] Park KS, Ni Z, Côté AP, Choi JY, Huang R, Uribe-Romo FJ et al.[2006] Exceptional chemical and thermal stability of zeolitic imidazolate frameworks, Proceedings of the National Academy of Sciences, 103:10186-10191
[11] J Li, D Luo, C Yang, S He, S Chen, J Lin, et al.[2013] Copper (II) imidazolate frameworks as highly efficient photocatalysts for reduction of CO_2 into methanol under visible light irradiation, Journal of Solid State Chemistry, 203:154-159.
[12] MS Shaharun, S Shaharun, NA Zabidi, MF Taha.[2012]Effect of zirconia on the physicochemical properties of Cu/ZnO/Al2O3 catalyst, in American Institute of Physics Conference Series, 117-121.
[13] García-Benjume M, Espitia-Cabrera M, Contreras-García M. [2012]Enhanced Photocatalytic Activity of Hierarchical Macro-Mesoporous Anatase by Incorporation, International Journal of Photoenergy,
[14] JA Knowles, MJ Hudson.[1995] Preparation and characterisation of mesoporous, high surface area zirconium (IV) oxides, Journal of the Chemical Society, Chemical Communications, pp. 2083-2084.
[15] Arunkumar N, Sirajudeen KM. [2011] Approximate Entropy based ayurvedic pulse diagnosis for diabetics-a case study. In 3rd International Conference on Trendz in Information Sciences & Computing (TISC2011) (pp. 133-135). IEEE.
[16] Arunkumar N, Jayalalitha S, Dinesh S, Venugopal A, Sekar D. [2012] Sample entropy based ayurvedic pulse diagnosis for diabetics. In Advances in Engineering, Science and Management (ICAESM), 2012 International Conference on (pp. 61-62). IEEE.